Surface circulation of the eastern Mediterranean Levantine basin: Insights from analyzing 14 years of satellite altimetry data

Yael Amitai,[1] Yoav Lehahn,[1] Ayah Lazar,[1] and Eyal Heifetz[1]

Received 24 January 2010; revised 16 June 2010; accepted 8 July 2010; published 30 October 2010.

[1] The complex multiscale system circulation of the Levantine Eastern Mediterranean (EM) basin is analyzed by applying various spatiotemporal statistical methods on the AVISO 14 years (1993–2006) data set of satellite altimetry sea level anomalies. The Rossby deformation radius at the EM is at the order of 10 km, which is also the horizontal satellite resolution. Therefore, the geostrophic currents, derived from the satellite altimetry measurements, represent well the basin and the mesoscale circulations. The long-term averaged mean dynamic topography (MDT) is found to capture the different eddy activity regions in the EM; however, these regions are highly turbulent. The instantaneous currents in these regions can be different from the MDT-derived currents, by the same order of magnitude. Furthermore, the turbulence intensity appears to be nonperiodic, despite of the seasonal and long-term steric periodic variability. Because these eddies interact with the basin circulation flow, they modify it continuously. The major exception of this sporadic behavior is the Ierapetra eddy, southeast of Crete. It appears to be forced by shear of the summer Etesian winds, created when the Crete mountain ridges block these winds and cause a funneling effect. It has a persistent seasonal signature that dominates the variance of the entire Levantine basin.

Citation: Amitai, Y., Y. Lehahn, A. Lazar, and E. Heifetz (2010), Surface circulation of the eastern Mediterranean Levantine basin: Insights from analyzing 14 years of satellite altimetry data, *J. Geophys. Res.*, *115*, C10058, doi:10.1029/2010JC006147.

1. Introduction

[2] The surface circulation in the Levantine basin of the Eastern Mediterranean (EM) is a complex multiscale system [*Ozsoy et al.*, 1991; *Pinardi and Masetti*, 2000; *Fusco et al.*, 2003], characterized by areas with strong eddy kinetic energy (EKE) [*Robinson et al.*, 1987; *Pujol and Larnicol*, 2005; *Pascual et al.*, 2007]. Yet, despite its complexity, the eastern basin of the Mediterranean has not been explored as extensively as the western basin.

[3] A pioneering attempt to characterize the EM surface circulation was made by *Nielsen* [1912], who constructed a simplified scheme of the basin scale surface pattern, based on field campaigns. Subsequently, more in situ measurements were performed to characterize the basin scale circulation [*Ovchinnikov*, 1966; *Hecht et al.*, 1988; *Ozsoy et al.*, 1989; *Robinson et al.*, 1991]. Construction of more detailed circulation schemes, which also take into account the subbasin mesoscale patterns, became possible with the technological development of recent years such as: analysis of sequential satellite time series of sea surface temperature (SST) [*Matteoda and Glenn*, 1996; *Hamad et al.*, 2006] and sea surface height (SSH) [*Ayoub et al.*, 1998; *Larnicol et al.*, 2002; *Pascual et al.*, 2007; *Rio et al.*, 2007]; numerical model simulations [*Tziperman and Malanotte-Rizzoli*, 1991; *Lascaratos et al.*, 1993; *Pinardi and Masetti*, 2000; *Alhammoud et al.*, 2005]; and recently, a thorough field campaign was carried out, in the framework of the EGITTO/EGYPT program, [*Gerin et al.*, 2009], which used satellite-tracked drifters that were released in the Sicily channel as well as in areas of specific interest in the Levantine basin.

[4] Several aspects of the EM circulation are widely agreed upon. For example, a well agreed pattern of the EM circulation is the relatively fresh Atlantic water (AW) crossing the Sicilian channel to form the Ionian and the Levantine surface water. The AW flows eastward, becoming denser via evaporation exceeding precipitation, and sinks in specific northern zones to create deep and intermediate water masses [*Ovchinnikov*, 1966; *Hecht et al.*, 1988; *Theocharis et al.*, 1993].

[5] Other aspects of the EM circulation are still under debate. One of the major controversial issues is the main pathway of the incoming AW and the governing basin scale surface current: is it basin centered, or does it flow along seashore slopes? The concept of a basin centered governing current, is supported by the detailed, multi methodical research of the EM surface circulation conducted by the POEM (Physical Oceanography of the Eastern Mediterranean) group. Using multiple-ship surveys, intercalibrated data sets, cooperative analysis, syntheses, and modeling during the years 1985–1992 [*Ozsoy et al.*, 1989; *Robinson et al.*, 1991; *Robinson and Golnaraghi*, 1993; *Malanotte-Rizzoli et al.*, 1997], they suggested that the main feature

[1]Department of Geophysics and Planetary Sciences, Tel Aviv University, Tel Aviv, Israel.

0148-0227/10/2010JC006147

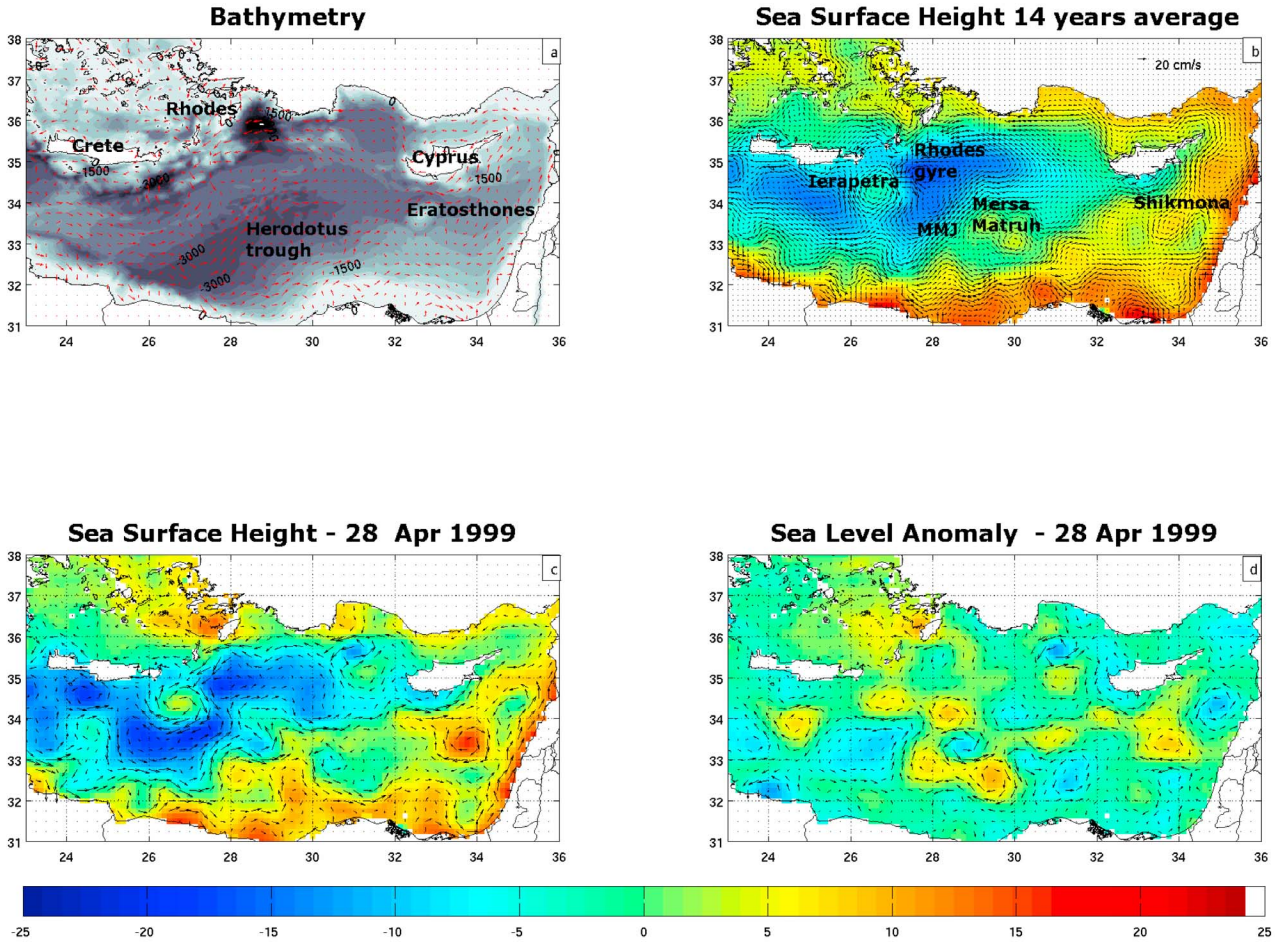

Figure 1. The Levantine basin (a) bathymetry (contours) and geostrophic velocity field calculated from 14 years averaged SSH (arrows); (b) 14 years averaged SSH (colors) with the corresponding geostrophic velocities (arrows) and the main "building block" eddies (see text); (c) SSH of a randomly chosen day; and (d) SLA of the same day, which is obtained by subtracting RIO 05 MDT from Figure 1c. The arrows mark the geostrophic velocities corresponding to the relevant altimetry field. The 14 years averaged SSH (Figure 1b) is almost identical to the MDT of the study by *Rio et al.* [2007], with a maximum difference of the order of 0.001 of the velocities.

in the Levantine basin is the Mid-Mediterranean Jet (MMJ), from which mesoscale features, as Mersa-Matruh and Shikmona, are delineated (Figure 1b). The alternative surface circulation scheme, the along-shore flow, suggested by *Hamad et al.* [2005], and completed by *Hamad et al.* [2006], was constructed by tracking of SST anomalies. Their results support the historical theoretic scheme suggested by *Nielsen* [1912] of an anticlockwise AW basin circulation, that results from the Coriolis force. This anticlockwise (cyclonic) circulation is assumed to be constrained along the coast by Kelvin waves associated with the basin wind stress [*Molcard et al.*, 2002], while anticyclonic eddies (e.g., Mersa-Matruhin Figure 1b) occupy the southern part of the basin and export AW seaward. This scheme is further supported by high-resolution XBT in situ measurements [*Fusco et al.*, 2003; *Zervakis et al.*, 2003] and by recent numerical simulations [*Alhammoud et al.*, 2005].

[6] Another issue which is under debate is the nature of the EM mesoscale circulation [*Millot and Taupier-Letage*, 2005]. Overall one can distinguish between two main approaches. The first [e.g., *Poem*, 1992; *Matteoda and Glenn*, 1996; *Rio et al.*, 2007] considers the Levantine circulation as composed of several distinct "building-block" eddies which can be permanent, recurrent, or propagating. These "building-block" eddies are the anticyclone Ierapetra, southeast of Crete; the anticyclone Mersa-Matruh, in the southern part of the basin; the cyclonic Rhodes gyre, which is an area of dense water formation; and the Shikmona anticyclone, near the northern coast of Israel (Figure 1). The customary terminology defines eddies as mesoscales that are not constrained by the bathymetry (but can be guided by it), and thus can grow and propagate, as opposed to gyres, that are larger circulation features, constrained by the bathymetry along most of their periphery, thus stationary for the most part [*Hamad et al.*, 2006]. The second approach [e.g., *Robinson et al.*, 1987; *Pujol and Larnicol*, 2005; *Pascual et al.*, 2007] considers the mesoscale flow as turbulent. Therefore, rather than tracking specific eddies, it char-

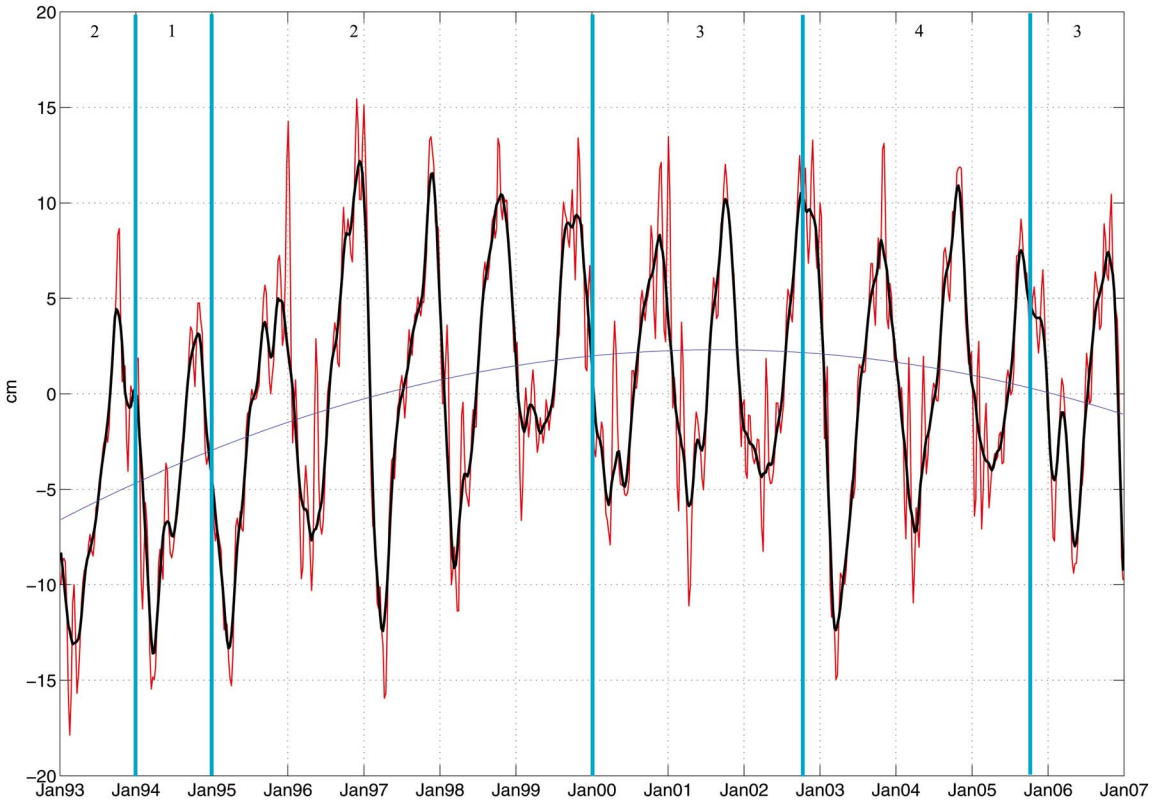

Figure 2. The 14 years (1993–2006) time series of SLA averaged over the Levantine basin of the of the eastern Mediterranean (red line) and smoothed with a 10 weeks running window (black line). The blue line marks the raw time series calculated trend. Data are considered reliable for high-resolution studies when it combines 2 or more missions [*Pascual et al.*, 2007] (number of available missions for different periods is indicated at the top).

acterizes regions in the basin according to the amount of eddy activity accumulated there (defined by *Hamad et al.* [2005] as ΣLE). The annual and interannual eddy activity variability is often quantified by the eddy kinetic energy (EKE). We note that both approaches indicate that there is more mesoscale activity in the Levantine basin than other parts of Mediterranean.

[7] This work addresses some of the ambiguities concerning our understanding of the Levantine basin surface circulation. This is done by analyzing the surface geostrophic velocity field derived from 14 years (1993–2006) of satellite altimetry data, using various spatiotemporal statistical methods. The satellite data, statistical methods and results are described in the next section, followed by conclusions.

2. Analysis and Results

[8] The study is based on the AVISO satellite altimetry data set of Sea surface height (SSH), for the years 1993–2006 (http://www-aviso.cnes.fr). The distributed regional product combines satellite altimetry data from the Topex/Poseidon, ERS, Jason-1, and Envisat missions. The number of missions merged into the final AVISO product ranges from 1 to 4 (Figure 2). The SSH weekly data are gridded on a (1/8° × 1/8°) regular grid. Sea level anomalies (SLA) are obtained by subtracting the Rio-05 Mean Dynamic Topography (MDT) [*Rio et al.*, 2007] from the SSH. The MDT is based on 7 years SSH averaging, combined with drifting buoy data and corrected from model outputs. The total and residual geostrophic currents are calculated, respectively, from the SSH and SLA, using a centered finite differences scheme. The derived geostrophic currents provide a decent representation of both the basin and the mesoscale circulations, since the horizontal sampling resolution is at the order of the Rossby internal radius of deformation (12 km in the EM).

[9] One may argue that the "eddy building-block" approach represents the average state of the mesoscale circulation. Indeed, when constructing the 14 years (1993–2006) averaged geostrophic currents, obtained from the SSH, these building blocks are clearly seen (Figure 1b). This long-term averaging is almost identical to the MDT presented by *Rio et al.* [2007] to the order of 0.001 of the mean velocities. Overall the MDT structure follows the varying basin bathymetry from the deep Herodotus trough in the west to the shallow Eratosthenes sea-mount in the east (Figure 1a). The extent to which this averaged picture represents the instantaneous mesoscale flow depends on the flow variability, or in other words, on its turbulent nature. Figure 1c represents a random weekly averaged snapshot which is quite different from Figure 1b. The Sea Level Anomaly (SLA) in Figure 1d, which is the instantaneous SSH minus the MDT (in fact, Figure 1c minus Figure 1b), is of the same order of magnitude as the MDT. Consequently,

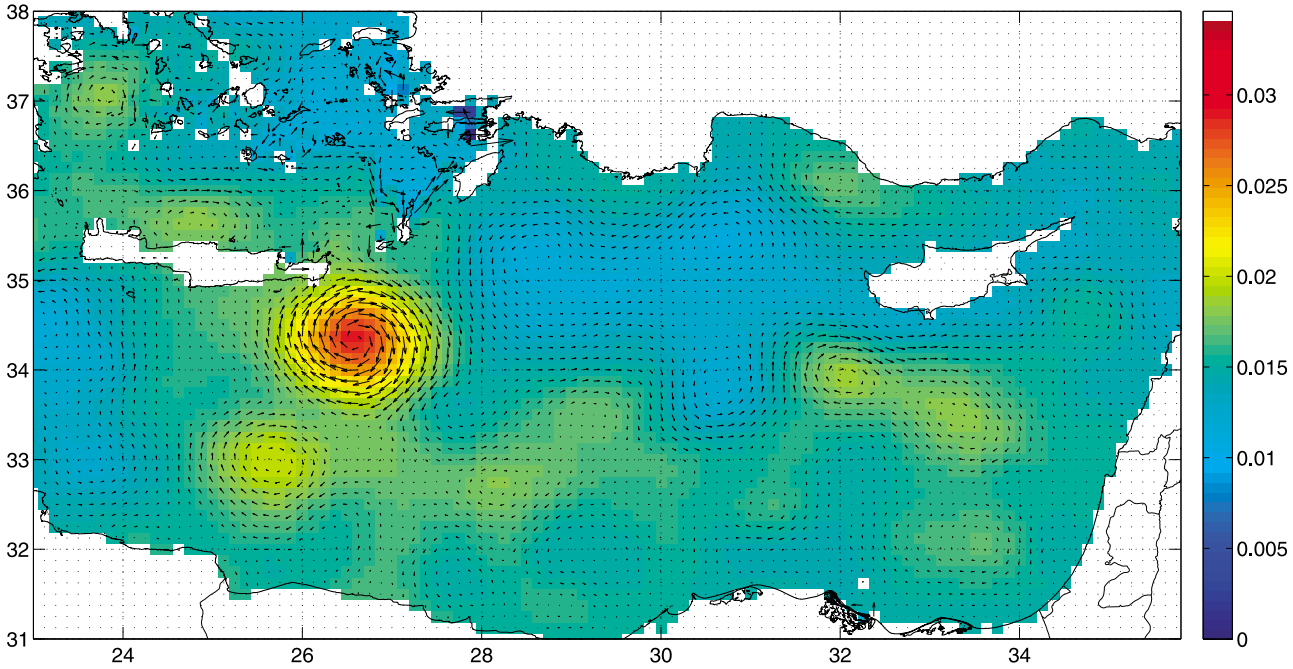

Figure 3. First spatial EOF mode (73.6%) of SLA (colors) and the corresponding geostrophic velocities (arrows).

the geostrophic current derived from the SLA and the MDT are of the same order of magnitude as well. This comparison suggests that at least some regions in the mesoscale circulation are indeed variant and that the "eddy building-block" description should be mainly applied when referring to the long-term averaged circulation.

[10] The 14 years evolution of SLA, when spatially averaged over the entire Levantine basin (23E-36E/31N-38N - adopting the definition of the Levantine basin of *Millot and Taupier-Letage* [2005]), is shown in Figure 2. The SLA signal displays a distinct seasonal cycle, with low values during spring and high values during fall. This seasonal cycle in SLA is also apparent from a Fast Fourier Transform (FFT) power spectrum analysis, which is not shown here.This is commonly explained by water column dilation and contraction, associated with seasonal change in the heat flux [*Ayoub et al.*, 1998; *Larnicol et al.*, 2002]. The interannual variation, apparent by the time series power spectrum as well, and the observed negative trend during the four last years of the data set are in agreement with *Cazenave et al.* [2002] and recently, with *Criado-Aldeanuevaa et al.* [2008].

[11] In order to examine the spatial nature of the Levantine surface circulation variability, we apply an Empirical Orthogonal Function (EOF) analysis on the SLA field. The first EOF, accounting for 73.6% of the total variance, is presented in Figure 3 (the second and the third modes are account for only 2.74% and 2.49% of the total variance, thus they are statistically insignificant). The most prominent feature in the first EOF is the strong Ierapetra anticyclone, southeast of Crete, however a careful look reveals features such as the Rhodes gyre and the anticyclone south of Ierapetra (which might be a different appearance of Ierapetra in several years [*Larnicol et al.*, 2002]). Contrasting Figure 3 with the MDT structure in Figure 1b, it is evident that only the Ierapetra can be regarded as a recurrent "building-block eddy".

[12] EOF analysis indeed tends to intensify signature of stationary eddies, but to smear signature of propagating eddies. Therefor next, we look at the Eddy Kinetic Energy (EKE) time series and Hovmoller diagram to examine the spatiotemporal nature of these propagating eddies.

[13] The geostrophic current anomalies are proportional to the horizontal derivatives of the SLA [$\mathbf{u}'_g = (g/f)\hat{\mathbf{k}} \times \nabla\eta$, where $\mathbf{u}'_g$ is the geostrophic current anomalies, g is gravity, f is the Coriolis parameter, $\hat{\mathbf{k}}$ is the perpendicular unit vector, and η is the SLA]. The horizontal derivative of the basin steric effect (which is the spatial average over η, $\langle\eta\rangle$) that is indicated in Figure 2, is zero. Therefore the anomalies should not be directly affected by the basin seasonal variations.

[14] The basin's EKE is characterized by a distinct annual cycle (Figures 4a–4b), and a distinct, but weaker, half-annual signal. A decadal variability is also evident in the Levantine basin's time series. In order to examine this variability in detail we look at the time series, and its corresponding power spectrum, of the five most energetic subregions that contribute mostly to the total basin EKE, as defined in *Rio et al.* [2007]. These are the 1 × 1 degree subregions of Ierapetra (centered at 27E/34.3N), Rhodes gyre (28E/34.5N), Mersa-Matruh (29.5E/33N), Shikmona (33.8E/33.5N) and the Mid Mediterranean jet (MMJ), which is calculated upon inclined rectangle of the same area (28E/32.75N - 28.25E/34N). The mean EKE values of these regions are 272, 98, 106, 88, 151 cm^2/sec^2, respectively (compared to the basin mean value of 126.5 cm^2/sec^2). The power spectrum of the most energetic region, Ierapetra (Figures 4c–4d), is dominated by an annual signal, although there is also a signal at 1.5 1/yr. However, its decadal variability is absent or even opposite to the basin trend. The power spectrum of the EKE signal over the Rhodes gyre

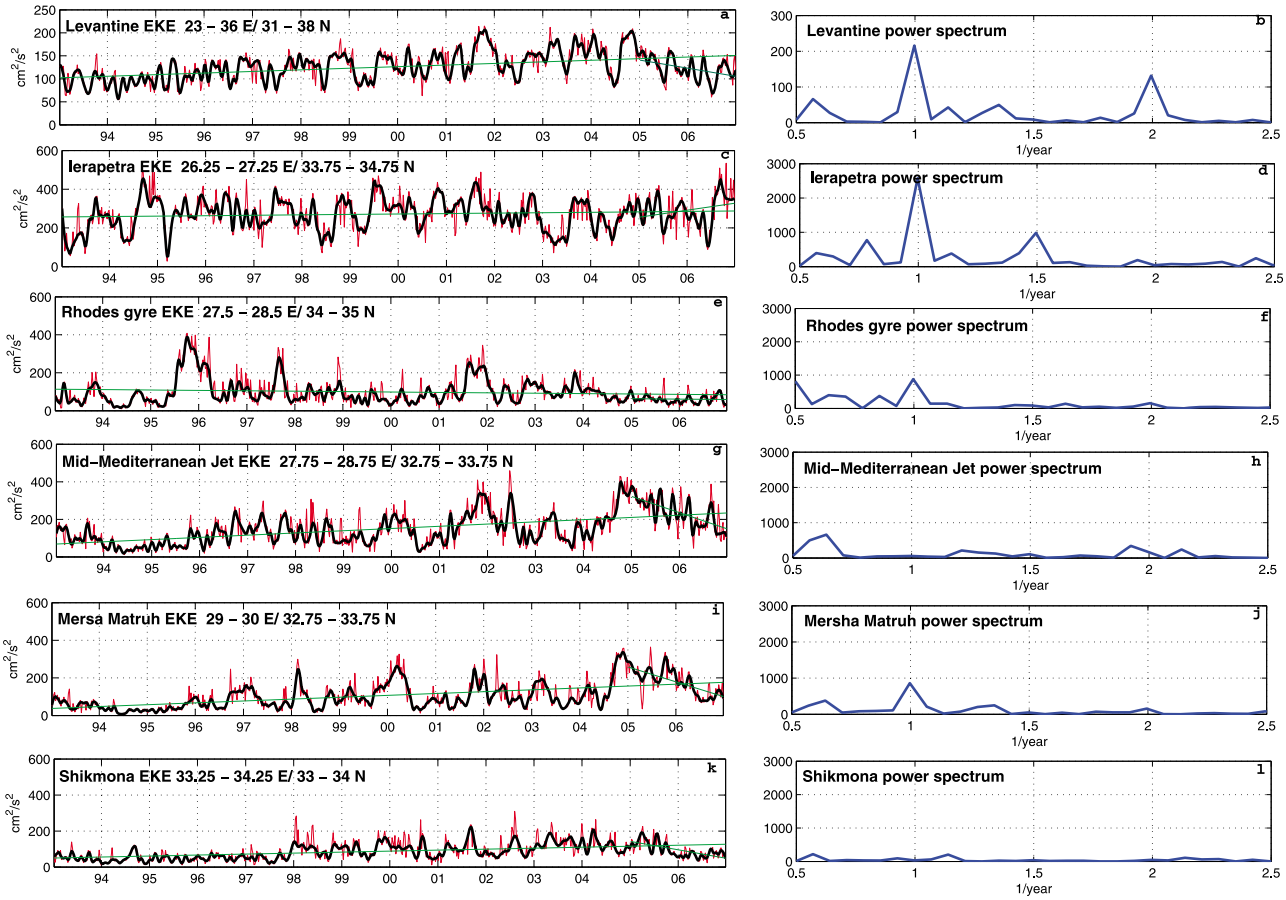

Figure 4. Time series of EKE averaged and its corresponding power spectrum, over the (a and b) entire Levantine basin; and a 1° × 1° area around (c and d) Ierapetra, (e and f) Rhodes gyre, (g and h) mid-Mediterranean jet, (i and j) Mersa-Matruh, and (k and l) Shikmona. Notice the different scales used for the whole basin and the rest of the features; this is because of the difference in the averaged area. The red line is the original signal, and the black line is the result of smoothing with a 10 weeks running window. Green lines represent the positive and negative trends in each time series. Note that the power spectra's axis starts at 0.5 1/yr to remove aliasing effect of the FFT.

(Figure 4f) and Mersa-Matruh (Figure 4j) subregions, show an annual signal as well, although far less distinct (note that the averaged area for these regions are the same, and therefore comparable). The EKE signals over the MMJ (Figure 4g) and Mersa-Matruh (Figure 4i) subregions seem to have a similar behavior throughout the years, and a similar decadal variability, which indicates their dynamical relationship. Furthermore, the MMJ's signal appears to have several identical elements as the basin signal and shares a resemblance to its interannual variability. Hence, the Ierapetra seasonal EKE signal variability dominates the entire basin, while the decadal variability may be due to the MMJ and Mersa-Matruh eddy-mean flow system (furthermore, the normalized correlation coefficient between these two EKE time series is 0.88).

[15] The Hovmoller diagram, in Figure 5, is a compact way to present the spatiotemporal variability in the different regions of the basin. The diagram in Figure 5a captures the northern part of the basin (computed by meridionally averaging each EKE image between 33.5°N and 35°N), including the subregions of Ierapetra and the Rhodes gyre. Similarly to the time series in Figure 4b, the Hovmoller diagram emphasizes the periodic nature, with higher values during fall and lower values in spring, and strong amplitude of the EKE signal, of Ierapetra subregion (marked by the dashed black line in Figure 5a). It also shows that the spatial nature of the Ierapetra EKE signature is remarkably stationary. The southern basin Hovmoller diagram in Figure 5b (computed by meridionally averaging EKE between 32°N and 33.5°N) includes the subregions of Mersa-Matruh and Shikmona. In the Mersa-Matruh area the signal is less periodic, with abrupt events of high EKE. It seems that eddies in this area originate further west and propagate eastward into the region as can be seen in Figure 5b (e.g., from the second half of 2003 to the end of 2004). Furthermore, there is high EKE values, between the years 1997–1999, south of Ierapetra, which might be accounted for the second appearance of the eddy, that was evident by the SLA first EOF, and was discussed previously by *Larnicol et al.* [2002].

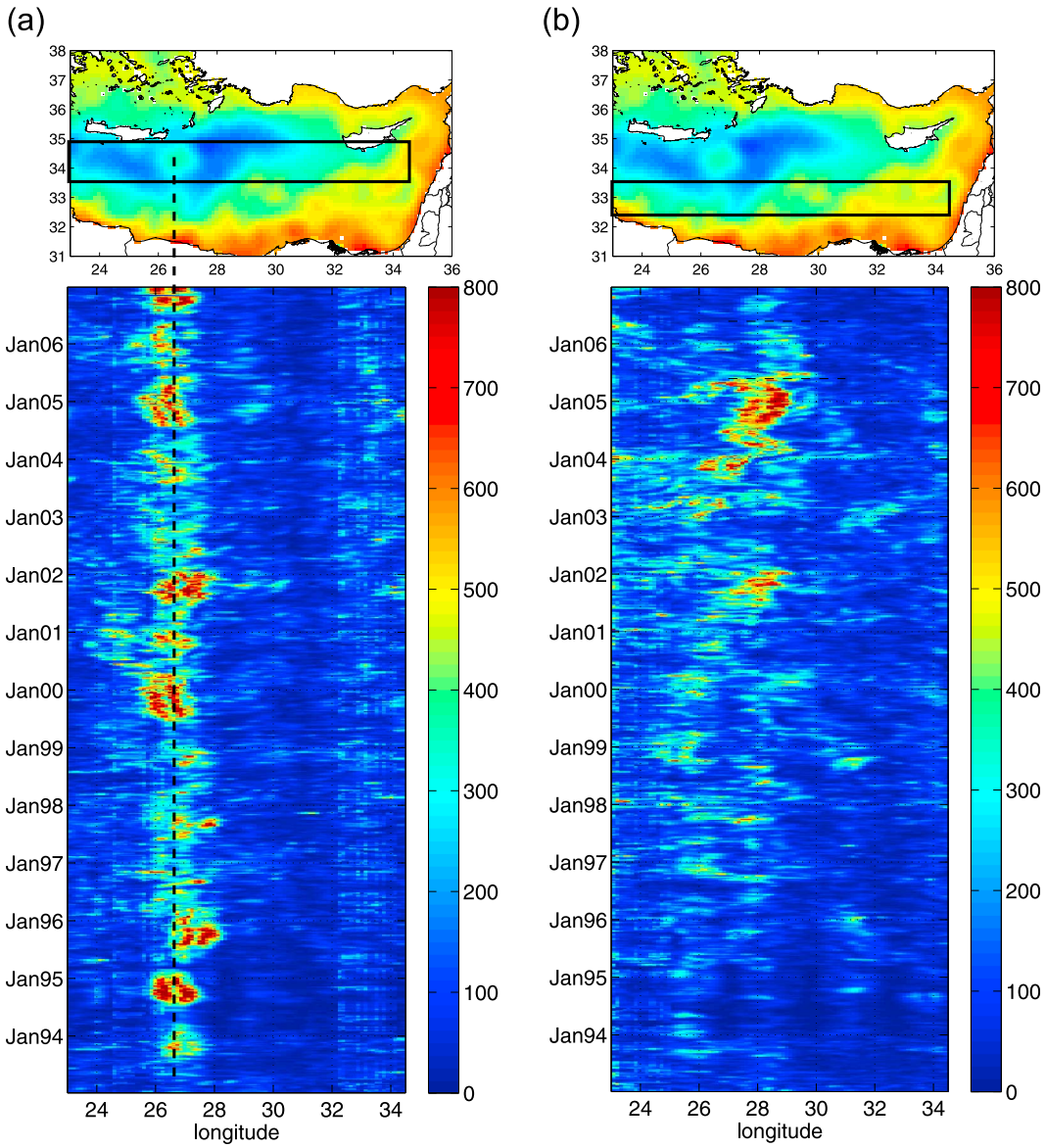

Figure 5. EKE Hovmoller diagrams over the (a) northern and (b) southern parts of the Levantine basin. The diagrams are extracted by averaging EKE meridionally between 33.5°N and 35°N and between 32°N and 33.5°N, respectively. Above are reference figures showing the averaged area. In Figure 5a, the dashed line marks the location of the Ierapetra eddy. In Figure 5b, the dashed lines mark the time in which snapshots of the Mersa-Matruh region are presented in Figure 7. The lower line corresponds to Figure 7a and the lower to Figure 7e.

[16] The debate regarding the governing basin scale circulation (along-shore versus basin centered) cannot be fully resolved by altimetry data, because the geostrophic assumption, used to derive the velocities, is insufficient close to shore. However, we are able to discuss the variability of the MMJ's flux and direction. In the MDT field (Figure 1b), the MMJ has a confined distinct structure in the border between Mersa-Matruh and the Rhodes gyre [mainly from south west (28E, 33N) to northeast (29E, 34N)]. Performing a time series analysis of the SSH velocity vector projection on the MMJ's defined direction, according to the MDT, shows that the MMJ's current is very variable in respect to the mean velocity in that subregion (Figure 6). Furthermore, it is nonperiodic in a seasonal time scale and dominated by abrupt changes, as the minimum in May 2002.

[17] This variability of the MMJ can be understood when considering the turbulent nature of the Mersa-Matruh region. In periods when Mersa-Matruh is active (high EKE values), as in the lower dashed line in Figure 5b, it is clear from the SLA derived currents of the same period (Figures 7a–7d) that the MMJ is intensified. This occurs due to the presence of coherent mesoscale anticyclones that propagate northeastward with an averaged speed of approximately 5 km/day. In contrast, in the periods of a low EKE signaling Mersa-Matruh (upper dashed line in Figure 5b), both cyclonic and anticyclonic eddies are less coherent and tend to weaken the MMJ significantly (see Figures 7e–7h). The correlation

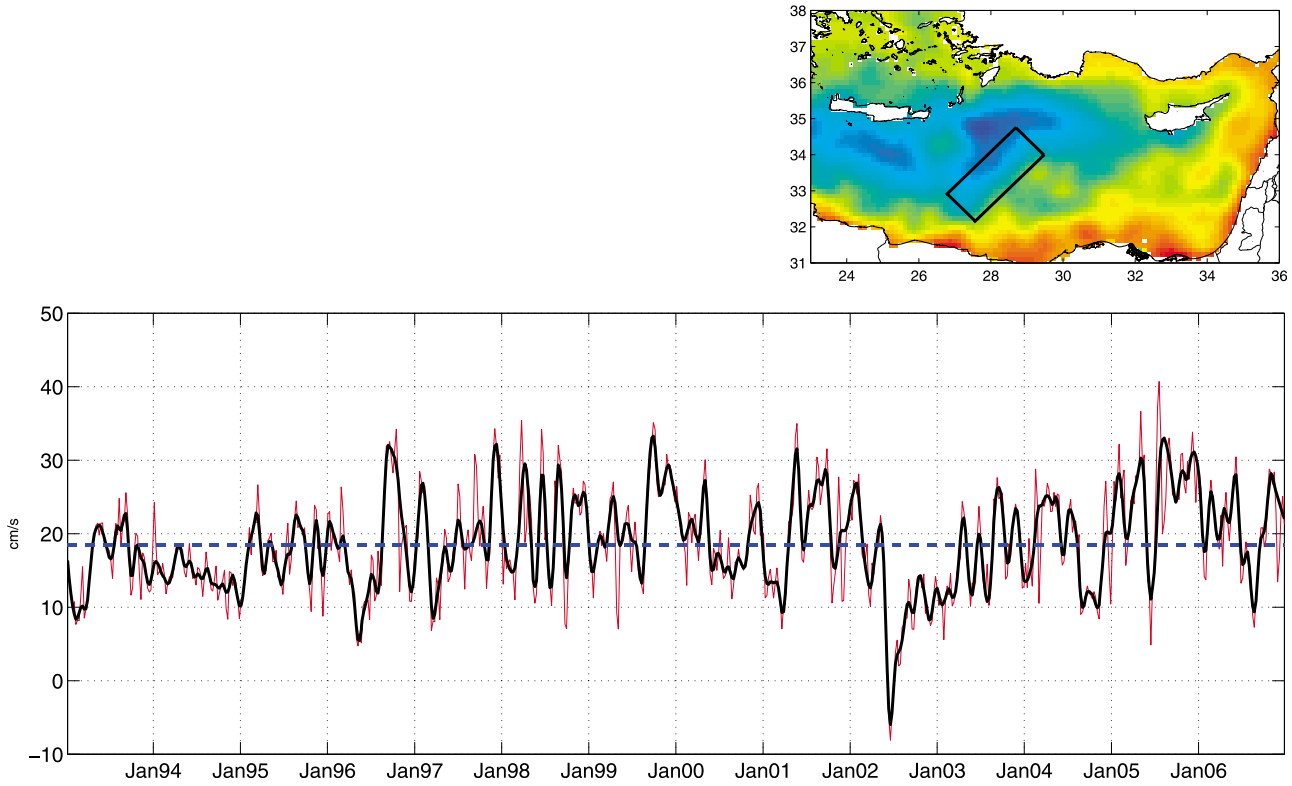

Figure 6. Time series of the geostrophic anomalies velocity vector projection on 45°, where the MMJ appears on the MDT, with a reference figure above. The red line is the original signal, and the black line is the result of smoothing with a 10 weeks running window. The blue dashed line is the mean value of the geostrophic velocity calculated from the SSH in the MMJ subregion.

between the MMJ strength and Mersa-Matruh's presence is also apparent from Figures 4g and 4i, where large EKE values in the Mersa-Matruh subregion indicate a high eddy activity. SLA derived currents in the Shikmona subregion (Figure 8) showing periods characterized by one persistent, but rather weak, anticyclonic eddy(Figures 8a–8d) versus other periods characterized by a conglomeration of cyclones and anticyclones (Figures 8e–8f). The snapshots in Figures 7 and 8 are taken in following seasons when four satellite missions are merged (Figure 2). As noted by *Pascual et al.* [2007], three altimeters are sufficient for tracking mesoscale features.

[18] Hence, the only region in the Levantine basin showing a persistent mesoscale signature on annual time scale is the Ierapetra eddy. The Ierapetra formation and strength have been connected to the MMJ position [*Theocharis et al.*, 1993], to the Aegean water outflow [*La Violette et al.*, 1998] and to Rhodes gyre energy [*Popov*, 2004]. In 1994 ? suggested that it results mainly due to atmospheric forcing. In summer time the Crete island (which is characterized by three high mountain ridges, crossing the island from west to east, and reaching altitudes of more than two kilometer) tends to block the Etesian south-eastward winds, thus causing a funneling effect of the wind through the Kasos strait. Therefore, although the large-scale Etesian winds are cyclonic, the wind blockade at Crete yields a localized negative sheared wind stress curl in the Ierapetra subregion (Figure 9). The interannual variability of the Etasian winds explains the interannual variability of Ierapetra. Horton's hypothesis has been supported by the inability of oceanic general circulation models to reproduce Ierapetra without considering a fine resolution of atmospheric forcing [*Marullo et al.*, 2003; *Nittis et al.*, 2003; *Alhammoud et al.*, 2005]. The seasonal variability of the Etasian winds and Ierapetra is correlated with an average lag of three month, between maximum negative wind stress curl and maximum negative sea current vorticity, in the Ierapetra subregion. This might be associated with the typical growth rate of the first baroclinic mode there.

3. Conclusions

[19] One of the major advantages of satellite altimetry is in providing continuous, synoptic, detailed data sets on the scale of a decade. Such long data sets compliment in situ short-term field campaigns, data from released drifters and buoys, and SST images which are frequently contaminated by cloud coverage. The analyzed data set in this study is particularly refined since the EM is covered by at least two satellite altimeters in thirteen out of the fourteen years of data (in three years it is covered by three altimeters and in other three years, it is covered by four). Furthermore, since the SLA horizontal sampling resolution is of the order of the Rossby internal radius of deformation the derived geostrophic currents resolve the mesoscale eddies.

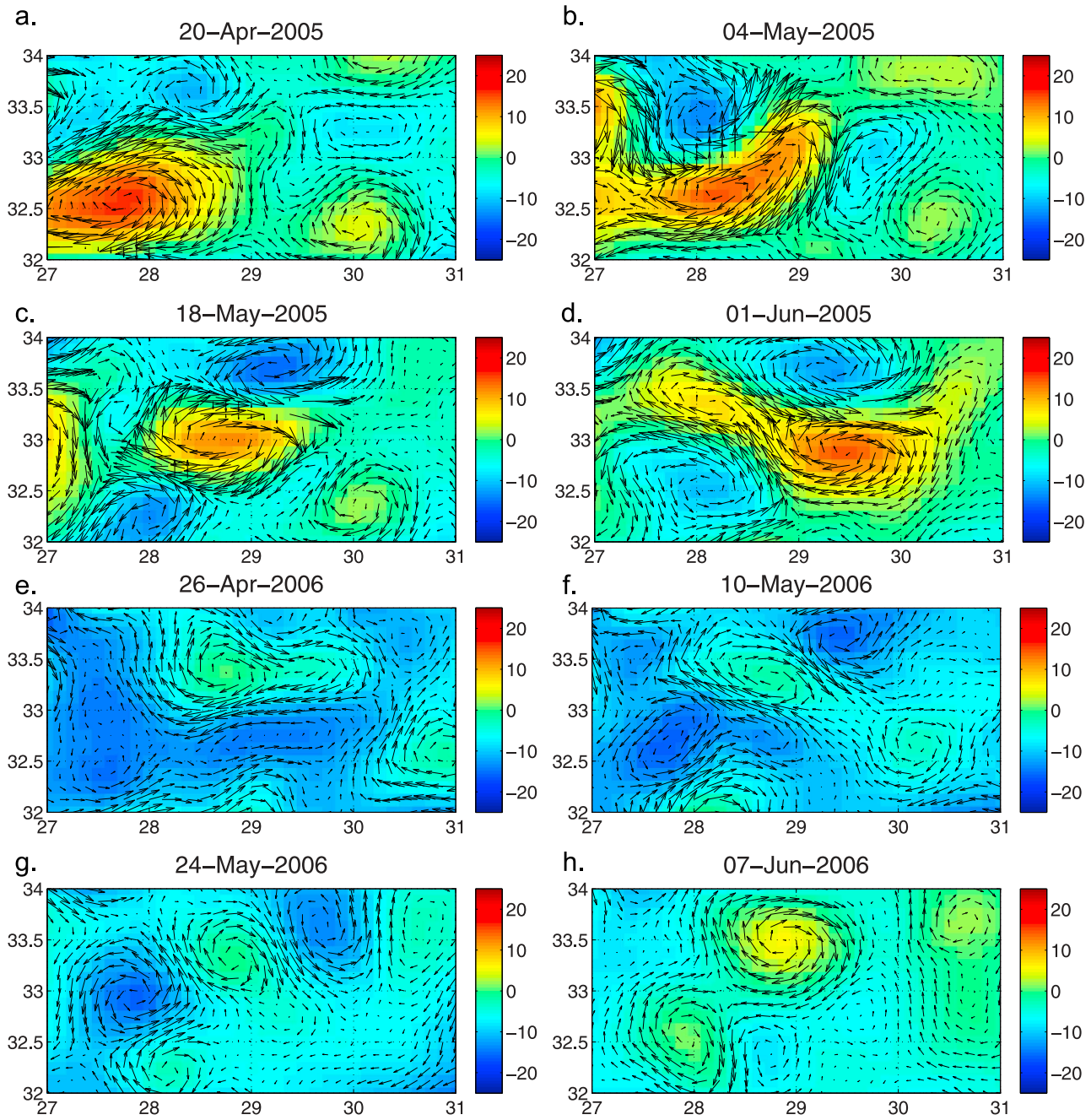

Figure 7. Evolution of SLA (colors) and the corresponding geostrophic velocities (arrows) in Mersa-Matruh region (32°N–34°N/27°–31°) during the spring (April–May) of (a–d) 2005 and (e–h) 2006. Notice that in Figures 7a–7d, there is one distinguishable anticyclonic eddy that propagate eastward, and the SLA-derived velocity field has a large contribution to the MMJ's defined direction. However, in Figures 7e–7h, there is no one traceable eddy but a conglomeration of cyclones and anticyclones that change rapidly, and there is not much contribution to the MMJ.

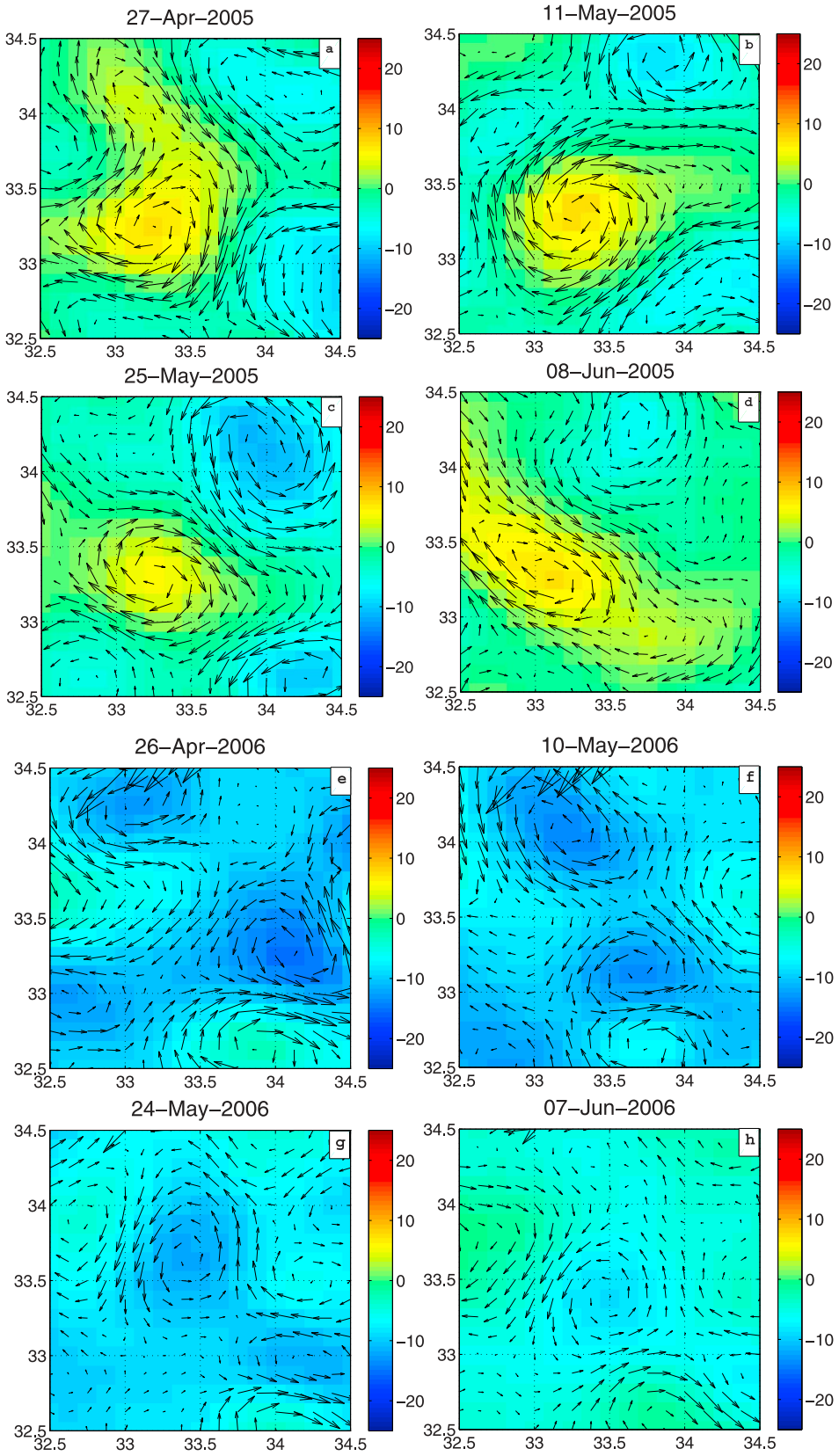

Figure 8. Evolution of SLA (colors) and the corresponding geostrophic velocities (arrows) in Shikmona region (32.5°N–34.5°N/32.5°E–34.5°E) during the spring (April–May) of (a–d) 2005 and (e–h) 2006. Notice that in Figures 8a–8d, there is one distinguishable persistent anticyclonic eddy. However, in Figures 8e–8h, there is no one traceable eddy but a conglomeration of cyclones and anticyclones that change rapidly.

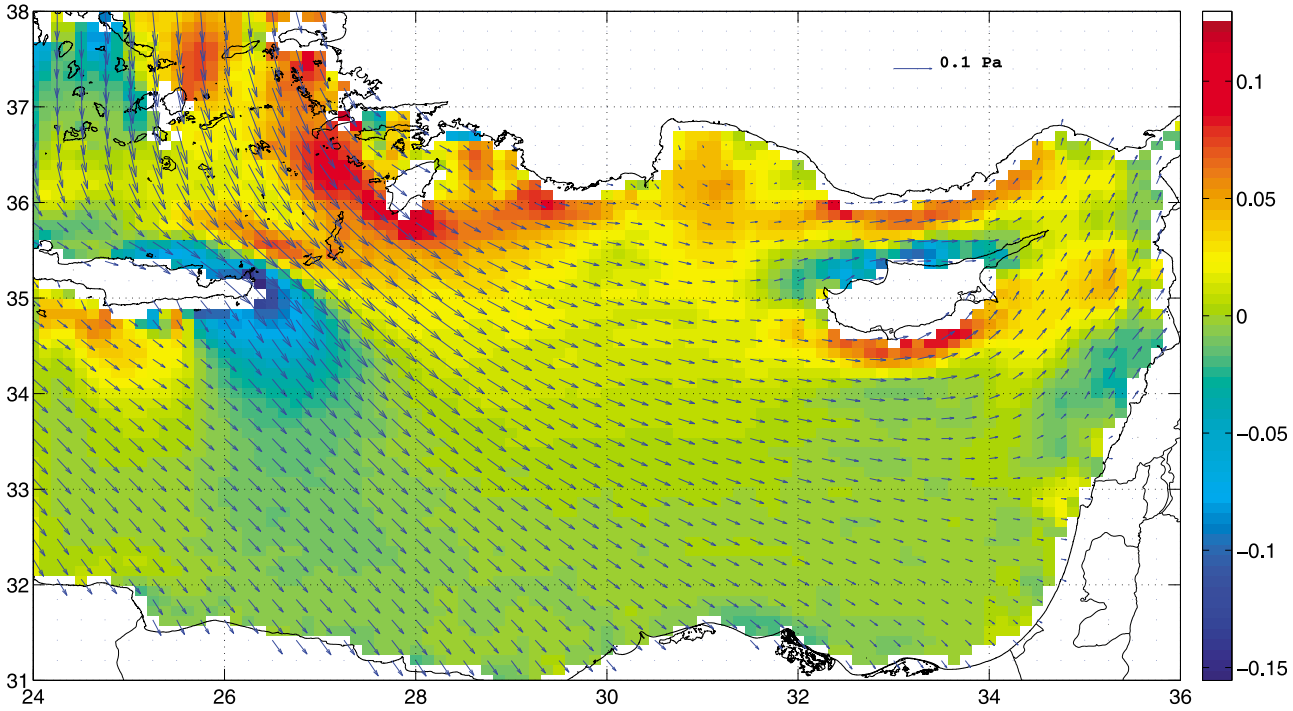

Figure 9. Summertime (July–August) wind stress (arrows) and wind stress curl (colors) over the Levantine basin. Note the wind stress curl minima over the Ierapetra region (southeast of Crete). Surface wind speeds were obtained from the SeaWinds scatterometer on board NASA's Quick Scatterometer (QuikSCAT) satellite. QuikSCAT data were obtained through the on line PO.DAAC Ocean ESIP Tool (POET) at the Physical Oceanography Distributed Active Archive Center (PO.DAAC), NASA Jet Propulsion Laboratory, Pasadena, California (available at http://podaac.jpl.nasa.gov/poet).

[20] The main finding from analyzing 14 years of data set is that the MDT picture represents correctly the different eddy activity regions in the Levantine, however these regions are turbulent regions and characterized by sporadic events. Furthermore, the instantaneous currents in these regions can be different from the MDT derived currents by the same order of magnitude. The turbulence intensity is highly variable, despite of the seasonal and long-term steric periodicity. Since these eddies interact with the basin circulation flow they modify it continuously. This basically means that in a given day one can find cyclones in averagely anticyclonic regions such as Mersa Matruh and Shikmona. Although the debate regarding the main pathway of Atlantic water in the Levantine basin, cannot be fully resolved by altimetry (since the nongeostrophic along shore current cannot be derived by altimetry), the existence of the MMJ can be ascertained (in line with *Alhammoud et al.* [2007]). Analysis reveals that the MMJ continuously transports AW into the basin, with a rather strong flux (averaged speed of 19 cm/sec). However, it meanders and its strength changes rapidly as a function of the variability of the eddy activity regions that surround it. This variability might explains the contradiction in the literature, concerning the prominent role of the MMJ.

[21] The prominent exception of this sporadic picture is the Ierapetra eddy with persistent seasonal appearance and location. This persistence seems to result from the persistence of the eddy deriving Etesian winds, which result themselves from the far field influence of the summer Indian Monsoon on the EM. The Ierapetra eddy dominates the mesoscale annual variance of the Levantine basin, while the eddy-mean flow system of Mersa-Matruh and the MMJ dominates its mesoscale decadal variance.

[22] **Acknowledgments.** The altimeter products were produced by the CLS (Collecte Localisation Satellites) Space Oceanography Division and distributed by Aviso with support from Cnes (http://www.aviso.oceanobs.com). We are grateful to Francesco d'Ovidio for providing the software and for fruitful discussion. We also thank the Israeli Science Foundation (ISF 1084/06) and to the Israeli Ministry of Science and Technology (MOST 3-6490) for funding this research.

References

Alhammoud, B., K. Branger, L. Mortier, M. Crpon, and I. Dekeyser (2005), Surface circulation of the Levantine Basin: Comparison of model results with observations, *Prog. Oceanogr.*, *66*, 299–320.

Alhammoud, B., K. Branger, L. Mortier, I. Dekeyser, and M. Crpon (2007), Does the mid-Mediterranean jet exist?, *Rapp. Comm. Int. Mer Mdit.*, *38*, 123.

Ayoub, N., P. Y. Le Traon, and P. De Mey (1998), A description of the Mediterranean surface variable circulation from combined ERS-1 and TOPEX/POSEIDON altimetric data, *J. Mar. Syst.*, *18*, 3–40.

Cazenave, A., P. Bonnefond, F. Mercier, K. Dominh, and V. Toumazou (2002), Sea level variations in the Mediterranean Sea and Black Sea from satellite altimetry and tide gauges, *Global Planet. Change*, *34*(1–2), 59–86.

Criado-Aldeanuevaa, F., J. Del Ro Verab, and J. Garca-Lafuente (2008), Steric and mass-induced mediterranean sea level trends from 14 years of altimetry data, *Global Planet. Change*, *60*(3–4), 563–575.

Fusco, G., et al. (2003), Variability of mesoscale features in the Mediterranean Sea from XBT data analysis, *Ann. Geophys.*, *21*(1), 21–32.

Gerin, R., P. Poulain, I. Taupier-Letage, C. Millot, S. Ben Ismail, and C. Sammari (2009), Surface circulation in the Eastern Mediterranean using drifters (2005–2007), *Ocean Sci. Discuss.*, *6*, 525–555.

Hamad, N., C. Millot, and I. Taupier-Letage (2005), A new hypothesis about the surface circulation in the eastern basin of the Mediterranean Sea, *Prog. Oceanogr.*, *66*(2–4), 287–298.

Hamad, N., C. Millot, and I. Taupier-Letage (2006), The surface circulation in the eastern basin of the Mediterranean Sea as inferred from infrared images, *Sci. Mar.*, *70*, 457–503.

Hecht, A., N. Pinardi, and A. Robinson (1988), Currents, water masses, eddies and jets in the Mediterranean Levantine basin, *J. Phys. Oceanogr.*, *18*, 1320–1353.

La Violette, P. E., J. A. Price, R. Mosher, and N. Kotsovinos (1998), The surface circulation around crete inferred from satellite imagery, drifter buoy, AXBTS data and a physical model, *Rapp. Comm. Int. Mer Medit.*, *35*, 162–163.

Larnicol, G., P. Y. Ayoub, and N. Le Traon (2002), Major changes in Mediterranean Sea level variability from 7 years of TOPEX/Poseidon and ERS-1/2 data, *J. Mar. Syst.*, *33–34*, 63–89.

Lascaratos, A., R. G. Williams, and E. Tragou (1993), A mixed-layer study of the formation of Levantine Intermediate Water, *J. Geophys. Res.*, *98*(C8), 14,739–14,750, doi:10.1029/93JC00912.

Malanotte-Rizzoli, P., et al. (1997), A synthesis of the Ionian Sea hydrography, circulation and water mass pathways during POEM-Phase I, *Prog. Oceanogr.*, *39*, 153–204.

Marullo, S., E. Napolitano, R. Santoleri, B. Manca, and R. Evans (2003), Variability of rhodes and Ierapetra gyres during Levantine intermediate water experiment: Observations and model results, *J. Geophys. Res.*, *108*(C9), 8119, doi:10.1029/2002JC001393.

Matteoda, A., and S. Glenn (1996), Observations of recurrent mesoscale eddies in the eastern Mediterranean, *J. Geophys. Res.*, *101*(C9), 20,687–20,709, doi:10.1029/96JC01111.

Millot, C., and I. Taupier-Letage (2005), Circulation in the Mediterranean Sea, in *The Handbook of Environmental Chemistry*, vol. 5, edited by A. Saliot, pp. 29–66, Springer, Heidelberg.

Molcard, A., N. Pinardi, M. Iskandarani, and D. B. Haidvogel (2002), Wind driven general circulation of the mediterranean sea simulated with a spectral element ocean model, *Dyn. Atmos. Oceans*, *35*(2), 97–130.

Nielsen, J. (1912), Hydrography of the Mediterranean and adjacent waters, *Tech. Rep. 1*, Rep. Dan. Ocean. Exp. Medit.

Nittis, K., A. Lascaratos, and A. Theocharis (2003), Dense water formation in the aegean sea: Numerical simulations during the eastern Mediterranean transient, *J. Geophys. Res.*, *108*(C9), 8120, doi:10.1029/2002JC001352.

Ovchinnikov, I. (1966), Circulation in the surface and intermediate layers of the Mediterranean, *Oceanology*, *6*, 48–59.

Ozsoy, E., A. Hecht, and U. Unluata (1989), Circulation and hydrography of the Levantine basin. results of poem coordinated experiments 1985–1986, *Prog. Oceanogr.*, *22*, 125–170.

Ozsoy, E., A. Hecht, U. Unluata, S. Brenner, T. Oguz, J. Bishop, M. Latif, and Z. Rozentraub (1991), A review of the Levantine basin circulation and variability during 1985–1988, *Dyn. Atmos. Oceans*, *15*, 421–456.

Pascual, A., M. Pujol, G. Larnicol, M. Le Traon, and P. Y. Rio (2007), Mesoscale mapping capabilities of multisatellite altimeter missions: First results with real data in the Mediterranean Sea, *J. Mar. Syst.*, *65*(1–4), 190–211.

Pinardi, N., and E. Masetti (2000), Variability of the large-scale general circulation of the Mediterranean Sea from observations and modeling: A review, *Palaeogeogr. Palaeoclimatol. Palaeoecol.*, *158*(21), 153–173.

Poem, G. (1992), General circulation of the Eastern Mediterranean, *Earth Sci. Rev.*, *32*, 285–309.

Popov, Y. I. (2004), Genesis and structure of the anticyclonic Ierapetra zone in the Levantine basin, *Prog. Oceanogr.*, *14*(4), 234–242.

Pujol, M.-I., and G. Larnicol (2005), Mediterranean sea eddy kinetic energy variability from 11 years of altimetric data, *J. Mar. Syst.*, *58*(3–4), 121–142.

Rio, M., P. Poulain, A. Pascual, E. Mauri, G. Larnicol, and R. Santoleri (2007), a mean dynamic topography of the Mediterranean Sea computed from altimetric data, in situ measurements and a general circulation model, *J. Mar. Syst.*, *65*(1–4), 484–508.

Robinson, A., and M. Golnaraghi (1993), Circulation and dynamics of the Eastern Mediterranean Sea; Quasi-synoptic data-driven simulations., *Deep Sea Res.*, *40*(6), 1207–1246.

Robinson, A., A. Hecht, N. Pinardi, J. Bishop, W. Leslie, Z. Rosentroub, A. Mariano, and S. Brenner (1987), Small synoptic/mesoscale eddies and energetic variability of the eastern Levantine basin, *Nature*, *327*, 131–134.

Robinson, A., M. Golnaraghi, W. Leslie, A. Artegiani, A. Hecht, E. Lazzoni, A. Michelato, E. Sansone, A. Theocharis, and U. Onliiata (1991), The eastern Mediterranean general circulation: Features, structure and variability, *Dyn. Atmos. Oceans*, *15*, 215–240.

Theocharis, A., D. Georgopoulos, A. Lascaratos, and K. Nittis (1993), Water masses and circulation in the central region of the Eastern Mediterranean: Eastern Ionian, South Aegean and Northwest Levantine, 1986–1987, *Deep Sea Res.*, *40*, 1121–1142.

Tziperman, E., and P. Malanotte-Rizzoli (1991), The climatological seasonal circulation of the Mediterranean Sea, *J. Mar. Res.*, *49*, 411–434.

Zervakis, V., G. Papadoniou, C. Tziavos, and A. Lascaratos (2003), Seasonal variability and geostrophic circulation in the eastern Mediterranean as revealed through a repeated XBT transect, *Ann. Geophys.*, *21*, 33–47.

Y. Amitai, E. Heifetz, A. Lazar, and Y. Lehahn, Department of Geophysics and Planetary Sciences, Tel Aviv University, Tel Aviv 69978, Israel. (yaelamit@post.tau.ac.il)